Bioorganic & Medicinal Chemistry Letters 23 (2013) 3592–3598

Contents lists available at SciVerse ScienceDirect

Bioorganic & Medicinal Chemistry Letters

journal homepage: www.elsevier.com/locate/bmcl

Novel triazolo-pyrrolopyridines as inhibitors of Janus kinase 1

Christopher A. Hurley [a,*], Wade S. Blair [g], Richard J. Bull [a], Christine Chang [g], Peter H. Crackett [a], Gauri Deshmukh [d], Hazel J. Dyke [a], Rina Fong [f], Nico Ghilardi [e], Paul Gibbons [c], Peter R. Hewitt [a], Adam Johnson [g], Tony Johnson [a], Jane R. Kenny [d], Pawan Bir Kohli [g], Janusz J. Kulagowski [a], Marya Liimatta [g], Patrick J. Lupardus [f], Robert J. Maxey [a], Rohan Mendonca [c], Raman Narukulla [a], Rebecca Pulk [c], Savita Ubhayakar [d], Anne van Abbema [g], Stuart I. Ward [a], Bohdan Waszkowycz [b], Mark Zak [c]

[a] Department of Medicinal Chemistry, Argenta, 8/9 Spire Green Centre, Harlow, Essex CM19 5TR, United Kingdom
[b] Department of Computer Aided Drug Design, Argenta, 8/9 Spire Green Centre, Harlow, Essex CM19 5TR, United Kingdom
[c] Department of Discovery Chemistry, Genentech, Inc., 1 DNA Way, South San Francisco, CA 94080, United States
[d] Department of Drug Metabolism and Pharmacokinetics, Genentech, Inc., 1 DNA Way, South San Francisco, CA 94080, United States
[e] Department of Immunology, Genentech, Inc., 1 DNA Way, South San Francisco, CA 94080, United States
[f] Department of Structural Biology, Genentech, Inc., 1 DNA Way, South San Francisco, CA 94080, United States
[g] Department of Biochemical and Cellular Pharmacology, Genentech, Inc., 1 DNA Way, South San Francisco, CA 94080, United States

ARTICLE INFO

Article history:
Received 22 February 2013
Revised 5 April 2013
Accepted 6 April 2013
Available online 17 April 2013

Keywords:
Janus kinase
JAK1
JAK2
JAK1 inhibitor

ABSTRACT

The identification of a novel fused triazolo-pyrrolopyridine scaffold, optimized derivatives of which display nanomolar inhibition of Janus kinase 1, is described. Prototypical example **3** demonstrated lower cell potency shift, better permeability in cells and higher oral exposure in rat than the corresponding, previously reported, imidazo-pyrrolopyridine analogue **2**. Examples **6**, **7** and **18** were subsequently identified from an optimization campaign and demonstrated modest selectivity over JAK2, moderate to good oral bioavailability in rat with overall pharmacokinetic profiles comparable to that reported for an approved pan-JAK inhibitor (tofacitinib).

Cytokine signaling pathways mediate a broad range of biological functions, including many aspects of inflammation and immunity.[1] Types I and II cytokine receptors lack kinase activity and instead transmit their signals through the receptor-associated Janus kinases (JAK1, JAK2, JAK3, and TYK2).[2,3] When stimulated, cytokine receptor complexes activate specific combinations of JAKs in well-defined patterns,[4] leading to further activation of signal transducer and activator of transcription (STAT) proteins residing in the cytoplasm. Upon JAK-mediated tyrosine phosphorylation, the STATs dimerise and are translocated to the nucleus where they regulate transcription of specific target genes.[5,6] Because of the importance of the JAK/STAT pathways in cytokine signaling, targeting of JAK kinases is envisioned to be useful in the treatment of a variety of diseases including rheumatoid arthritis (RA),[7] myeloproliferative disorders[8] and cancer.[9]

Current evidence suggests that immuno-relevant cytokines (such as IL-6 and the γ_c cytokines) play a pivotal role in RA disease pathogenesis.[10,11] The approved pan-JAK inhibitor tofacitinib (**1**, Fig. 1) has undergone extensive evaluation for RA and has demonstrated efficacy in various clinical trials, likely due to its suppression of the IL-6 and γ_c cytokine pathways.[12] Additionally, a humanized monoclonal antibody (tocilizumab) targeting the IL-6 pathway has been approved for the treatment of moderate to severe RA.[13] Although IL-6 activates JAK1, JAK2, and TYK2, knockout studies in mice have demonstrated that JAK1 plays a particularly important role in signal transduction.[14] Additionally, JAK1 has been shown to play a critical and potentially dominant role in the transduction of γ_c cytokine signaling.[15] Finally, inhibition of JAK2 is associated with anemia,[16] thus limiting its suppression may be beneficial. We, therefore, desired to develop potent JAK1 inhibitors with reduced inhibition of JAK2 to maximize anti-RA effects while limiting the potential for anemia.

We previously reported the identification and preparation of novel fused imidazo-pyrrolopyridine tricyclic JAK inhibitors, such as compound **2** (Fig. 1), that exhibited modest selectivity for JAK1 over the JAK2 isoform.[17] However, some members of this structural class were compromised by low in vitro permeability in MDCK cells and inadequate oral exposure in rat pharmacokinetic studies. In an effort to circumvent the problems faced with compounds such as **2**, we undertook an exploration to find suitable imidazo-pyrrolopyridine scaffold replacements. One restriction

* Corresponding author. Tel.: +44 1279 645 645; fax: +44 1279 645 646.
E-mail address: Chris.Hurley@glpg.com (C.A. Hurley).

0960-894X/$ - see front matter © 2013 Elsevier Ltd. All rights reserved.
http://dx.doi.org/10.1016/j.bmcl.2013.04.018

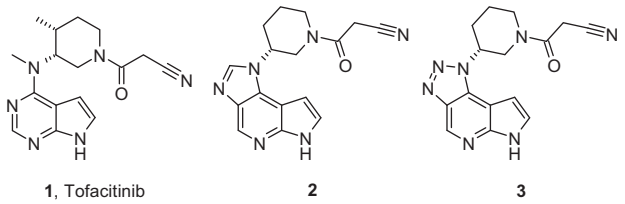

Figure 1. Structures of pan-JAK inhibitor tofacitinib **1**, imidazo-pyrrolopyridine **2** and triazolo-pyrrolopyridine **3**.

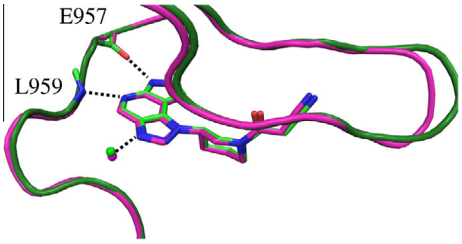

Figure 2. Comparison of the X-ray crystal structures of imidazo-pyrrolopyridine **2** (magenta: PDB code 4E6D) in complex with a JAK1-like JAK2 triple mutant[17] and triazolo-pyrrolopyridine **3** (green: PDB code 4I5C) in complex with JAK1. Hydrogen bonds to the ligand are depicted with black dashed lines. Backbone hinge atoms contacting **3** are highlighted (E957 and L959). Notable crystallographic waters are denoted as spheres. The resolutions of the X-rays are 2.3 and 2.1 Å, respectively.

we applied was the need to readily transfer SAR to any new series identified to expedite progression of the new scaffolds. Therefore we limited our search to scaffolds which maintained the topology of the existing core (compound **2**). This search resulted in the identification of an alternative series of fused triazolo-pyrrolopyridine tricycles (e.g., **3**). When investigated in the JAK1 biochemical assay, compound **3** exhibited similar, albeit slightly weaker, potency compared to **2** (Table 1). Since the measured pK_a of **3** was lower than the pK_a of compound **2**, we were concerned that this reduced basicity would be detrimental to the hydrogen bonding interactions with the hinge residues (JAK1 residues E957 and L959). Consequently, we obtained an X-ray co-crystal structure of **3** bound to JAK1 and compared it to an X-ray co-crystal structure of **2** bound to a JAK1-like JAK2 triple mutant (Fig. 2).[17] We were pleased to find that both the topology and the binding mode remained consistent between the two scaffolds, indicating that major SAR differences between the series would be unlikely.

Compound **3** displayed dramatically improved apical to basolateral MDCK permeability compared to **2**. This improved permeability likely contributes to the observed reduction in the cell potency shift and superior cell potency. Consistent with the imidazo-pyrrolopyridine scaffold, the triazole **3** demonstrated intrinsic but modest selectivity over JAK2 in both the biochemical and cell-based assays. Having shown a dramatic in vitro cell permeability advantage, we decided to explore the SAR of this new chemotype with the aim of improving selectivity against the JAK2 isoform while ensuring favorable JAK1 potency in cells (Table 2). Synthetic intermediate **4** exhibited modest biochemical potency and this prompted us to prepare the less stereo-chemically complex 4-piperidine isomer **5**. Pleasingly, this compound demonstrated single digit nanomolar JAK1 potency, suggesting a preference for the 4-piperidine ring. Compound **5** also displayed comparable potency in the cell-based assay to **3**. However, analogues **4** and **5** suffered from poor metabolic stability in human liver microsomes. We believed that the sub-optimal metabolic profile was due to these weakly basic compounds possessing relatively high lipophilicity (*c* Log *D*). Therefore, in an attempt to improve microsomal stability, we prepared compounds **6**, **7** and **8** that contained substituents on the piperidine nitrogen designed to reduce lipophilicity (Log *D*). The inclusion of a cyanoethyl moiety (**6**) led to elevated metabolic stability along with enhanced biochemical potency and better JAK1 isoform selectivity in cells. Compound **7** had similar selectivity and human microsomal stability profile to compound **6**, but was slightly less potent. The introduction of the pyridine (**8**) was disfavored and we made no further attempts to include heterocyclic systems within this scaffold.

We were keen to identify additional structural features to improve selectivity against JAK2. Previous investigations within our laboratories demonstrated that substitution on the piperidine nitrogen with suitable α-amino amide groups afforded enhanced selectivity against JAK2.[17] Accordingly, the proline analogue **9** was prepared and exhibited 5.9-fold selectivity over the JAK2 enzyme. However, the relatively weak biochemical JAK1 potency (121 nM) was insufficient to warrant further characterization. An alternative approach we had previously discovered involved the introduction of a 4-methyl substituent on the piperidine ring.[17] When applied to this system, compounds **10** and **11** demonstrated improved selectivity over the JAK2 isoform in the biochemical assay. Biochemically, the cyanoethyl moiety was strongly disfavored (compare **6** with **10**) highlighting that this modification was incompatible with the previously established SAR. Conversely, compound **11** demonstrated adequate potency and selectivity in the cell-based assay accompanied by robust microsomal stability to justify further progression.

During the course of our investigations, routine screening of late stage intermediates meant that compound **12** was assessed for activity and exhibited preferential potency for JAK1 over JAK2. We have previously reported that hydrogen bonding elements within this region of the imidazole series can lead to enhanced selectivity profiles.[17] Therefore, we examined a number of additional analogues incorporating H-bond donor groups to probe this region for beneficial selectivity enhancements (compounds **13**–**24**). Fluorinated piperidines compounds **14** and **15** were designed to reduce the basicity of the piperidine nitrogen (ACD cpK_a: **12** = 9.7; **15** = 7.7)[18] and the *trans*-analogue (**15**) was

Table 1
Physicochemical and in vitro data for compounds **2** and **3**

Ex	JAK1 K_i[a,b] (nM)	JAK2 K_i[a,b] (nM)	JAK1 cell EC_{50}[a,c] (nM)	JAK1 cell selectivity[d]	JAK1 cell potency shift[e]	MDCK A:B P_{app}[f] ($\times 10^{-6}$ cm/s)	Log *D*[g]	pK_a (measured)
2	0.4	1.2	180	4.8	450	0.3	0.39	4.34
3	1.5	3.8	114	6.8	76	3.7	0.60	1.96

[a] Arithmetic mean of at least three separate determinations.
[b] Biochemical potency.
[c] pSTAT3-IL6 JAK1 driven TF-1 cell-based assay.
[d] Cell-based selectivity for JAK1 over JAK2 (pSTAT5-EPO EC_{50}/pSTAT3-IL6 EC_{50}).
[e] Fold reduction in cell potency relative to biochemical potency (pSTAT3-IL6 EC_{50}/JAK1 K_i).
[f] Apparent permeability in MDCK transwell culture (arithmetic mean of at least two separate determinations), A:B apical to basolateral.
[g] Measured at pH 7.2.

Table 2
Biological data and physicochemical properties for compounds **4–24**

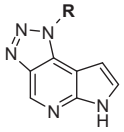

Ex	R	JAK1 K_i[a,b] (nM)	JAK2 K_i[a,b] (nM)	JAK1 enzyme selectivity[c]	JAK1 cell EC_{50}[a,d] (nM)	JAK1 cell selectivity[e]	HLM $T_{1/2}$[f] (h)	Log D[g] (c Log D)
4	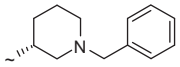	25[h]	40	1.6×	ND	ND	0.2	ND (2.5)
5	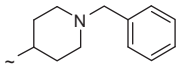	8.5	15	2.0×	121	3.4×	0.5	ND (2.3)
6	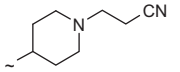	2.1	3.7	1.8×	138	4.6×	1.9	1.12
7	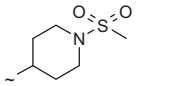	6.2	12	1.9×	249	4.8×	1.7	1.05
8	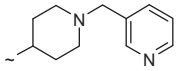	16	28	1.7×	414	2.7×	0.7	2.03
9	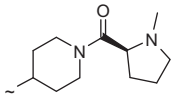	121	721	5.9×	ND	ND	1.1	ND (−1.2)
10	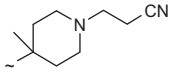	156	487	3.1×	ND	ND	4.8	1.92
11	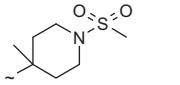	7.9	53	6.7×	220	15×	32	1.50
12	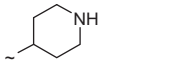	210	669	3.2×	ND	ND	ND	−0.35
13	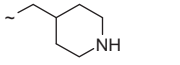	745	1232	1.7×	ND	ND	1.3	ND (−1.6)
14[i]	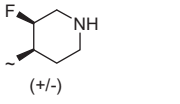 (+/-)	198	446	2.3×	ND	ND	ND	0.27
15[i]	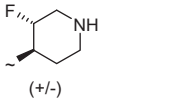 (+/-)	21	57	2.7×	ND	ND	15	0.77
16	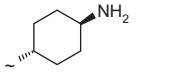	21	121	5.8×	729	7.9×	1.1	−0.24
17	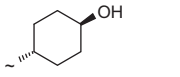	12	32	2.7×	558	4.2×	1.2	1.76
18	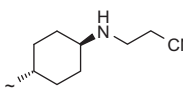	5.9	21	3.6×	165	6.7×	2.3	1.05
19	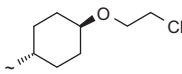	>3763	ND	ND	ND	ND	5.8	1.36
20	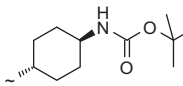	120	401	3.3×	ND	ND	1.0	3.58

Table 2 (*continued*)

Ex	R	JAK1 K_i[a,b] (nM)	JAK2 K_i[a,b] (nM)	JAK1 enzyme selectivity[c]	JAK1 cell EC_{50}[a,d] (nM)	JAK1 cell selectivity[e]	HLM $T_{1/2}$[f] (h)	Log D[g] (*c* Log D)
21	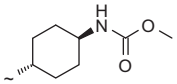	12	27	2.3×	433	4.0×	4.8	2.08
22	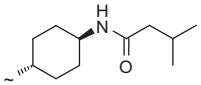	4.7	17	3.6×	350	5.0×	3.7	2.7
23[j]	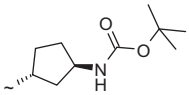	2.4	10	4.2×	127	4.3×	0.9	3.53
24[i]	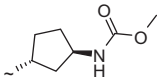 (+/-)	12	33	2.8×	395	6.8×	4.3	1.98

ND = not determined.
[a] Arithmetic mean of at least three separate determinations.
[b] Biochemical potency.
[c] Biochemical selectivity for JAK1 over JAK2 (JAK2 K_i/JAK1 K_i).
[d] pSTAT3-IL6 JAK1 driven TF-1 cell-based assay.
[e] Cell-based selectivity for JAK1 over JAK2 (pSTAT5-EPO EC_{50}/pSTAT3-IL6 EC_{50}).
[f] Half-life in the presence of in vitro preparations of human liver microsomes.
[g] Measured at pH 7.2 or calculated (*c* Log D) at pH 7.2 see Ref. 18 for details.
[h] Biochemical determination $N = 2$.
[i] Racemate.
[j] Single enantiomer.

Table 3
In vitro and rat pharmacokinetic profiles of compounds **3**, **6**, **7**, **11** and **18**

Ex	Kinase selectivity[b] (>40% inhibition)	JAK1 cell potency shift[c,d]	MDCK A:B P_{app}[d,e] ($\times 10^{-6}$ cm/s)	In vivo rat PK[a,f]			
				F[d] (%)	C_{max}[d] (μM) (po)	AUC[d] (μM h) (po)	CL[d,g] (mL/min/kg)
3	0/50	76 (450)	3.7 (0.3)	41 (5)	0.4 (0.05)	1.0 (0.3)	110 (85)
6	ND	66 (72)	17 (8.5)	28 (48)	4.9 (1.8)	1.8 (1.6)	44 (96)
7	ND	40 (120)	13 (1.6)	>100 (36)	4.6 (2.9)	18 (2.3)	16 (45)
11	0/50	28 (123)	14 (2.5)	82 (74)	0.7 (0.8)	1.0 (2.3)	211 (82)
18	1/50	28 (98)	7.2 (2.3)	44 (28)	0.9 (0.6)	1.4 (0.7)	88 (120)

ND = not determined.
[a] PK data are the mean profiles from three animals.
[b] Number of enzymes inhibited >40% out of a panel of 50 non-JAK kinases, at a test concentration of 100× JAK1 K_i.
[c] Fold reduction in cell potency relative to biochemical potency (pSTAT3-IL6 EC_{50}/JAK1 K_i).
[d] Values in parentheses correspond to imidazo-pyrrolopyridine analogues reported in Ref. 17.
[e] Apparent permeability in MDCK transwell culture (arithmetic mean of at least two separate determinations), A:B apical to basolateral.
[f] PK data normalized to 1 mg/kg iv and 5 mg/kg po.
[g] Plasma clearance following iv dosing.

10-fold more potent biochemically than **12**. Unfortunately, the increased structural complexity coupled with the poor reactivity of the piperidine nitrogen prevented a meaningful follow-up campaign around compound **15**. The introduction of a methylene spacer between the tricyclic core and the piperidine ring (**13**) was strongly disfavored. Whereas when the H-bonding moiety was relocated (**16**) this resulted in enhanced potency (compared to **12**) with slightly improved selectivity. Preparation of the corresponding *cis* isomer was not undertaken as previous investigations found this was disfavored.[17] Compound **17**, possessing a hydroxyl group as a H-bond donor moiety, had similar potency to **16**, however the selectivity against the JAK2 isoform degraded in both the biochemical and cell-based assays. In an attempt to improve the potency of compound **16**, the amine moiety was capped with a cyanoethyl group (**18**) to reduce the basicity of the nitrogen (ACD cpK_a: **16** = 10.3; **18** = 8.2). This transformation led to enhanced biochemical and cell potency and was accompanied by greater microsomal stability. Furthermore, compound **18** maintained the same magnitude of cell selectivity against JAK2 as analogue **16**. Appending

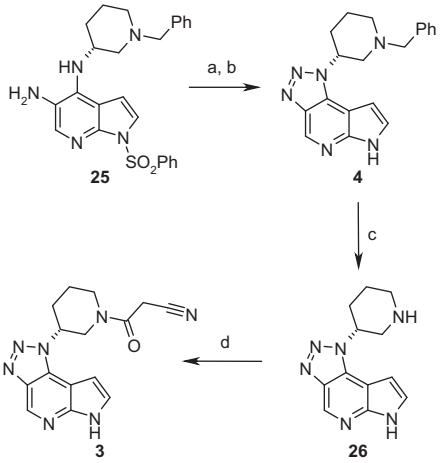

Scheme 1. Reagents and conditions: (a) *n*-Butyl nitrite, $CuBr_2$, CH_3CN, 70 °C, 2 h, 65% or sodium nitrite, AcOH, rt (ca. 95%); (b) NaOH (aq 2 M), MeOH/THF, 98%; (c) ammonium formate, $Pd(OH)_2$, MeOH, reflux, 91%; (d) cyanoacetic acid, HOBt, EDCI, DMAP, DCM, 92%.

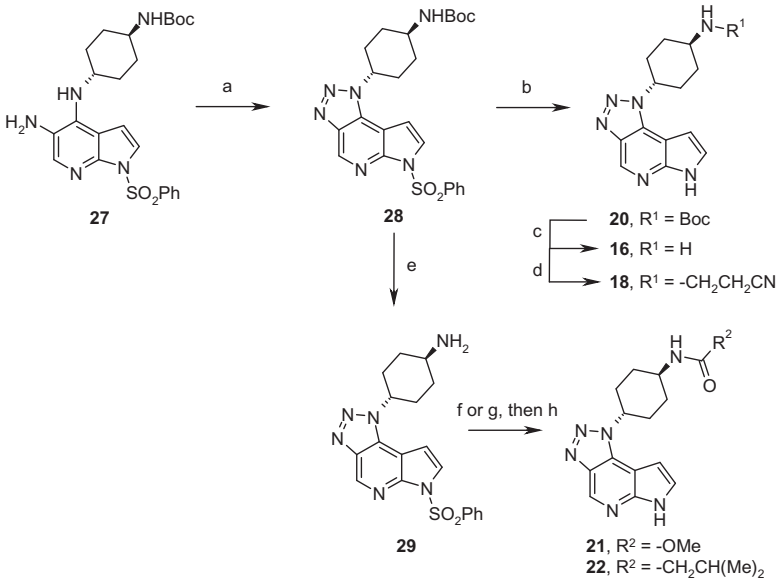

Scheme 2. Reagents and conditions: (a) sodium nitrite, AcOH, 45 min, rt, 99%; (b) NaOH (aq 2 M), MeOH, THF, rt, 1 h, 87%; (c) TFA, H_2O, rt, 2 h, 58%; (d) acrylonitrile, EtOH, reflux, 90 min, 18%; (e) TFA, H_2O, rt, 1 h, quantitative; (f) $ClCO_2Me$, iPr_2EtN, DCM, rt, 25 min, 90%; (g) $ClC(O)R^2$, iPr_2EtN, DMAP, DMF, rt, overnight; (h) NaOH (aq 1 M), MeOH, THF, rt, 45 min.

the cyanoethyl group to the alcohol (**19**) was not tolerated. With these results, we focused on identifying alternative substitutions to the cyanoethyl group found in **18**. Synthetic intermediate **20** was screened for biochemical potency at JAK1, and exhibited activity, albeit weak. We noted that this structural change was accompanied by reduced stability in human liver microsomes (compared to **18**). We attributed this reduction to an increase in the lipophilicity of the compound and this prompted us to prepare analogues which were more hydrophilic. The methyl carbamate **21** and amide **22** both demonstrated greater metabolic stability accompanied by improved biochemical potency. Disappointingly, both examples lacked sufficient potency in cells to justify further progression. We also investigated the effect of ring size on JAK1 potency. Accordingly, cyclopentane analogue **23** was prepared, and this displayed a ~50-fold improvement in biochemical potency (compared to **20**) with favorable cell potency. Despite the marginally reduced lipophilicity of **23**, poor metabolic stability was observed. Therefore, we deployed an analogous strategy to ease microsomal turnover within the cyclopentane system, and truncated the *tert*-butyl moiety to generate methyl carbamate **24**. Although stability in human liver microsomes improved, **24** exhibited reduced biochemical potency.

Several compounds were subjected to further evaluation and their in vitro and rat pharmacokinetic profiles are summarized in Table 3. Compounds **3**, **11**, and **18** were screened in JAK3 and TYK2 biochemical assays and were found to be >10-fold less potent against those isoforms compared to JAK1.[19] To assess the kinase selectivity of this series, compounds **3**, **11** and **18** were screened against a panel of 50 non-JAK kinases at a concentration 100-fold higher than their JAK1 K_i values. Examples **3** and **11** demonstrated excellent selectivity against all non-JAK related enzymes in the panel; however, **18** exhibited some activity against protein kinase D1 (inhibition = 44%). Cell permeability determination in MDCK cells indicated that the triazole analogues had moderate to good permeability that was routinely better than the equivalent imidazoles. As a result, analogues **3**, **6**, **7**, **11** and **18** demonstrated a lower potency shift from biochemical to cell-based assays than their corresponding fused imidazole analogues. We next examined examples **3**, **6**, **7**, **11** and **18** in male Sprague–Dawley rat to determine whether the

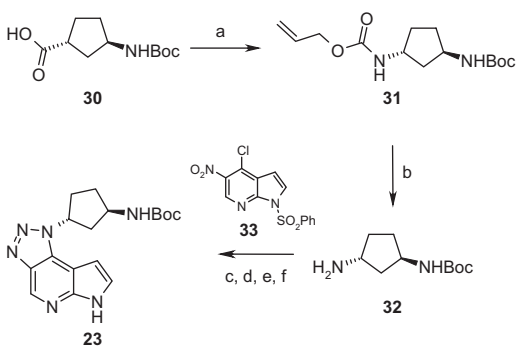

Scheme 3. Reagents and conditions: (a) DPPA, Et_3N, toluene, then allyl alcohol, DMAP, 72%; (b) 1,3-dimethylbarbituric acid, $Pd(PPh_3)_4$, DCM, reflux, 56%; (c) **33**, iPr_2EtN, propan-2-ol, reflux, 2 h, 88%; (d) Fe, NH_4Cl, MeOH, H_2O, reflux, quantitative; (e) sodium nitrite, AcOH, rt, 79%; (f) NaOH (aq 1 M), MeOH, THF, rt, 35%.

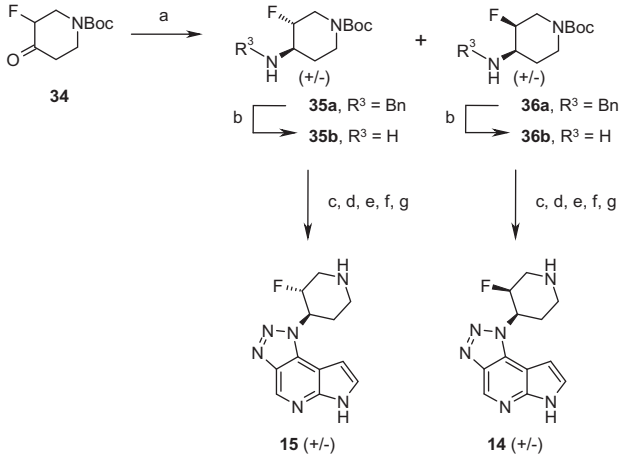

Scheme 4. Reagents and conditions: (a) $BnNH_2$, $NaCNBH_4$, MeOH, AcOH, rt, overnight, 30% (**35a**), 36% (**36a**); (b) H_2, 10% Pd on C, EtOAc; (c) **33**, iPr_2EtN, propan-2-ol, reflux; (d) H_2, 10% Pd on C, EtOAc; (e) sodium nitrite, AcOH; (f) TFA, DCM, 45 min; (g) NaOH (aq 1 M), EtOH, 60 °C, 2 h, 23% (**15**).

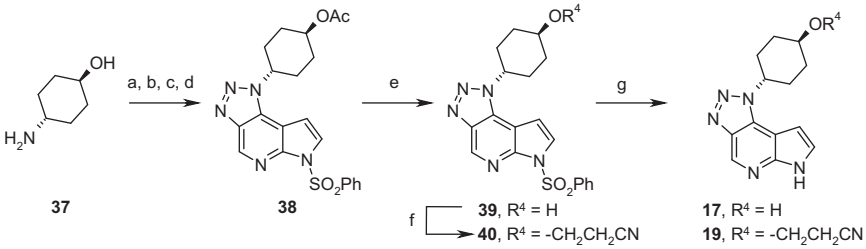

Scheme 5. Reagents and conditions: (a) **33**, iPr$_2$EtN, propan-2-ol, reflux, overnight, 96%; (b) acetyl chloride, iPr$_2$EtN, DMAP, DCM, rt, overnight; (c) Fe, NH_4Cl, MeOH, H_2O, reflux; (d) sodium nitrite, AcOH, rt, 45 min, 34% over three-steps; (e) LiOH (aq 1 M), THF, rt; (f) sodium hydride, MeCN, rt, then 3-bromopropionitrile, rt, overnight; (g) NaOH (aq 2 M), MeOH, rt, overnight, 84% (**17**) and 16% (**19**).

observed improvement in permeability would lead to improved oral exposure compared to the imidazole series. Analogues **3**, **7**, **11** and **18** exhibited superior oral bioavailabilities when benchmarked against their corresponding imidazole equivalents. Furthermore, compounds **6**, **7** and **18** also displayed lower plasma clearance following intravenous administration. Finally all compounds, except **11**, had higher oral AUC and C_{max} values. The extremely high clearance observed for compound **3** following iv dosing was reduced in compounds **6** and **7**. Conversely, compound **11** still showed exceptionally high clearance in vivo which prohibited further development of this compound. Overall, the rat pharmacokinetic profiles of compounds **3**, **6**, **7** and **18** compare favorably to that reported for the pan-JAK inhibitor tofacitinib (**1**).[20]

Preparation of the triazolo-pyrrolopyridine scaffold is outlined in Scheme 1.[21] The synthesis of key diamine intermediate **25** has been disclosed previously.[17] Cyclisation of **25** was achieved using either *n*-butyl nitrite/copper bromide or sodium nitrite in acetic acid. Subsequent cleavage of the sulfonyl protecting group under basic conditions furnished analogue **4**. Removal of the benzyl group was facile under transfer hydrogenation conditions affording amine **26** in good yield. Amine **26** was converted to analogue **3** using an EDCI-mediated coupling with cyanoacetic acid.

The syntheses of amino cyclohexane analogues **16**, **18**, **20**, **21**, and **22** are illustrated in Scheme 2. Cyclisation of diamino intermediate **27**,[17] using sodium nitrite, generated triazole **28**. Deprotection of the sulfonamide moiety furnished boc-protected amine **20** which was readily converted to amine **16** and then **18**. To prepare carbamate **21** and amide **22**, compound **16** could not be utilized as the competing di-acylation occurred. In the event, compounds **21** and **22** were best produced via boc-deprotection of intermediate **28** followed by amine derivatization and unmasking of the pyrrole nitrogen under basic conditions.

The synthesis of chiral cyclopentyl analogue **23** is summarized in Scheme 3. Commercially available amino acid **30** was converted to protected amine **31** utilizing a Curtius rearrangement. Deprotection of the allyl carbamate protecting group furnished **32**, which was subsequently coupled to intermediate **33**,[17] and progressed to analogue **23** using standard methodology. Preparation of racemic cyclopentyl analogue **24** utilized similar procedures as described herein and construction of racemic *trans*-diaminocyclopentane followed previously reported methodology.[22]

Fluorinated piperidines **14** and **15** were generated using the route illustrated in Scheme 4. Amines **35b** and **36b** were prepared according to literature procedures and were converted to triazole analogues **14** and **15** using established conditions.[23]

The route to analogues **17** and **19** is summarized in Scheme 5. Intermediate **38** was generated by reaction of **33** with 4-aminocyclohexanol (**37**), followed by protection of the alcohol moiety (acetyl), reduction of the nitro group, and subsequent cyclisation with sodium nitrite. Deprotection of **38** provided **39**, which was converted to analogue **17** under hydrolytic conditions. Intermediate **39** was alkylated with 3-bromopropionitrile to give **40**; subsequent unmasking of the pyrrole furnished analogue **19**.

In summary, we have identified a novel fused triazolo-pyrrolopyridine tricyclic scaffold which exhibited nanomolar JAK1 enzyme potency with intrinsic but modest selectivity against the JAK2 isoform and excellent selectivity against other non-JAK kinases. Representative compounds **3**, **7**, **11** and **18** demonstrated significantly improved in vitro permeability and better oral bioavailability compared to corresponding imidazo-pyrrolopyridine analogues.[17] Furthermore rat PK profiles for analogues **3**, **6**, **7** and **18** compared favorably to the reported profile of tofacitinib (**1**).[20]

Acknowledgments

We wish to thank Russell Scammell, Michael Podmore and Neil Bayliss for analytical support, Ning Liu (microsomal stability), Emile Plise and Jonathan Cheng (MDCK permeability) for in vitro ADME support, and Peter Dragovich for editorial assistance.

References and notes

1. (a) Tanaka, Y.; Iwata, S.; Yamaoka, K. *Inflamm. Regen.* **2011**, *31*, 237; (b) O'Shea, J. J.; Pesu, M.; Borie, D. C.; Changelian, P. S. *Nat. Rev. Drug Disc.* **2004**, *3*, 555; (c) Malemud, C. J.; Pearlman, E. *Curr. Signal Transduction Ther.* **2009**, *4*, 201.
2. Ghoreschi, K.; Laurence, A.; O'Shea, J. J. *Nat. Immunol.* **2009**, *10*, 356.
3. Kisseleva, T.; Bhattacharya, S.; Braunstein, J.; Schindler, C. W. *Gene* **2002**, *285*, 1.
4. Igaz, P.; Toth, S.; Falus, A. *Inflamm. Res.* **2001**, *50*, 435.
5. Leonard, W. J.; O'Shea, J. J. *Annu. Rev. Immunol.* **1998**, *16*, 293.
6. (a) Schindler, C.; Levy, D. E.; Decker, T. *J. Biol. Chem.* **2007**, *282*, 20059; (b) Levy, D. E.; Darnell, J. E., Jr. *Nat. Rev. Mol. Cell Biol.* **2002**, *3*, 651.
7. Stump, K. L.; Lu, L. D.; Dobrzanski, P.; Serdikoff, C.; Gingrich, D. E.; Dugan, B. J.; Angeles, T. S.; Albom, M. S.; Ator, M. A.; Dorsey, B. D.; Ruggeri, B. A.; Seavey, M. M. *Arthritis Res. Ther.* **2011**, *13*, R68.
8. (a) Quintas-Cardama, A.; Kantarjian, H.; Cortes, J.; Verstovsek, S. *Nat. Rev. Drug Disc.* **2011**, *10*, 127; (b) Verstovsek, S. *J. Clin. Oncol.* **2010**, *28*, 1; (c) Kiss, R.; Sayeski, P. P.; Keseru, G. M. *Expert Opin. Ther. Patents* **2010**, *20*, 471.
9. Brzezianska, E.; Domanska, D. *Curr. Signal Transduction Ther.* **2012**, *7*, 187.
10. O'Shea, J. J.; Husa, M.; Li, D.; Hofmann, S. R.; Watford, W.; Roberts, J. L.; Buckley, R. H.; Changelian, P.; Candotti, F. *Mol. Immunol.* **2004**, *41*, 727.
11. Malemud, C. J. *Anti-Inflammatory Anti-Allergy Agents Med. Chem.* **2011**, *10*, 78.
12. (a) West, K. *Curr. Opin. Invest. Drugs* **2009**, *10*, 491; (b) Kremer, J. M.; Bloom, B. J.; Breedveld, F. C.; Coombs, J. H.; Fletcher, M. P.; Gruben, D.; Krishnaswami, S.; Burgos-Vargas, R.; Wilkinson, B.; Zerbini, C. A. F.; Zwillich, S. H. *Arthritis Rheum.* **2009**, *60*, 1895; (c) FDA has approved tofacitinib for rheumatoid arthritis: <http://www.fda.gov/NewsEvents/Newsroom/PressAnnouncements/ucm327152.html>.
13. Scheinecker, C.; Smolen, J.; Yasothan, U.; Stoll, J.; Kirkpatrick, P. *Nat. Rev. Drug Disc.* **2009**, *8*, 273.
14. (a) Rodig, S. J.; Meraz, M. A.; White, J. M.; Lampe, P. A.; Riley, J. K.; Arthur, C. D.; King, K. L.; Sheehan, K. C. F.; Yin, L.; Pennica, D.; Johnson, E. M., Jr.; Schreiber, R. D. *Cell* **1998**, *93*, 373; (b) Shimoda, K.; Kato, K.; Aoki, K.; Matsuda, T.; Miyamoto, A.; Shibamori, M.; Yamashita, M.; Numata, A.; Takase, K.; Kobayashi, S.; Shibata, S.; Asano, Y.; Gondo, H.; Sekiguchi, K.; Nakayama, K.; Nakayama, T.; Okamura, T.; Okamura, S.; Niho, Y.; Nakayama, K. *Immunity* **2000**, *13*, 561; (c) Parganas, E.; Wang, D.; Stravopodis, D.; Topham, D. J.; Marine, J.-C.; Teglund, S.; Vanin, E. F.; Bodner, S.; Colamonici, O. R.; van Deursen, J. M.; Grosveld, G.; Ihle, J. N. *Cell* **1998**, *93*, 385.
15. Haan, C.; Rolvering, C.; Raulf, F.; Kapp, M.; Druckes, P.; Thoma, G.; Behrmann, I.; Zerwes, H.-G. *Chem. Biol.* **2011**, *18*, 314.
16. (a) Fleischmann, R.; Cutolo, M.; Genovese, M. C.; Lee, E. B.; Kanik, K. S.; Sadis, S.; Connell, C. A.; Gruben, D.; Krishnaswami, S.; Wallenstein, G.; Wilkinson, B. E.;

Zwillich, S. H. *Arthritis Rheum.* **2012**, *64*, 617; (b) Frenzel, K.; Wallace, T. A.; McDoom, I.; Xiao, H. D.; Capecchi, M. R.; Bernstein, K. E.; Sayeski, P. P. *Exp. Cell Res.* **2006**, *312*, 2735; (c) Neubauer, H.; Cumano, A.; Muller, M.; Wu, H.; Huffstadt, U.; Pfeffer, K. *Cell* **1998**, *93*, 397.

17. Kulagowski, J. J.; Blair, W.; Bull, R. J.; Chang, C.; Deshmukh, G.; Dyke, H. J.; Eigenbrot, C.; Ghilardi, N.; Gibbons, P.; Harrison, T. K.; Hewitt, P. R.; Liimatta, M.; Hurley, C. A.; Johnson, A.; Johnson, T.; Kenny, J. R.; Kohli, P. B.; Maxey, R. J.; Mendonca, R.; Mortara, K.; Murray, J.; Narukulla, R.; Shia, S.; Steffek, M.; Ubhayakar, S.; Ultsch, M.; van Abbema, A.; Ward, S. I.; Waszkowycz, B.; Zak, M. *J. Med. Chem.* **2012**, *55*, 5901.
18. ACD/labs 2012 release (build 1996. 1 June 2012) was used to calculate cpK_a and *c* Log*D* values.
19. Biochemical potencies for **3**: JAK3 K_i = 24 nM and TYK2 K_i = 20 nM. Biochemical potencies for **11**: JAK3 K_i = 369 nM and TYK2 K_i = 234 nM. Biochemical potencies for **18**: JAK3 K_i = 122 nM and TYK2 K_i = 80 nM.
20. (a) Reported rat PK profile for **1**: CL = 62 mL/min/kg; *F* = 27%; C_{max} = 442 ng/mL; AUC (po) (normalized to 5 mg/kg) = 1.16 μM h. AUC was calculated in house using the reported values for CL and % *F*.; (b) Flanagan, M. E.; Blumenkopf, T. A.; Brissette, W. H.; Brown, M. F.; Casavant, J. M.; Shang-Poa, C.; Doty, J. L.; Elliott, E. A.; Fisher, M. B.; Hines, M.; Kent, C.; Kudlacz, E. M.; Lillie, B. M.; Magnuson, K. S.; McCurdy, S. P.; Munchhof, M. J.; Perry, B. D.; Sawyer, P. S.; Strelevitz, T. J.; Subramanyam, C.; Sun, J.; Whipple, D. A.; Changelian, P. S. *J. Med. Chem.* **2010**, *53*, 8468.
21. (a) Compounds **5**–**12** were prepared using either 4-amino-1-benzylpiperidine or 4-amino-4-methyl-1-benzylpiperidine adapting the procedures described in Ref. 17. (b) Preparation of 3-oxo-3-[(3*R*)-3-(pyrrolo[2,3-*b*][1,2,3]triazolo[4,5-*d*]pyridin-1(6*H*)-yl)piperidin-1-yl]propanenitrile (**3**): A stirred solution of **25** (300 mg, 0.65 mmol) in acetonitrile (6 mL) was treated with copper(II) bromide (174 mg, 0.78 mmol) and *n*-butyl nitrite (114 μL, 0.97 mmol) and then heated to 70 °C for 2 h. After cooling, the reaction was quenched by the addition of 1 M aqueous HCl solution (ca. 5 mL) and stirred for 5 min. The mixture was basified with saturated sodium hydrogen carbonate solution and extracted with ethyl acetate (3×). The combined extracts were washed with brine, dried with sodium sulfate and concentrated under vacuum to leave a brown residue. Purification by column chromatography on silica gel (gradient: 0–60% ethyl acetate in cyclohexane) gave 200 mg (65%) of 1-[(3*R*)-1-benzylpiperidin-3-yl]-6-(phenylsulfonyl)-1,6-dihydropyrrolo[2,3-*b*][1,2,3]triazolo[4,5-*d*]pyridine as a brown residue. MS (ESI): m+H = 473.5; ^{1}H NMR (400 MHz, $CDCl_3$) δ: 9.18 (s, 1H), 8.21 (m, 2H), 7.82 (d, *J* = 3.7 Hz, 1H), 7.57 (m, 1H), 7.53–7.46 (m, 2H), 7.30 (s, 5H), 6.75 (d, *J* = 3.7 Hz, 1H), 4.88 (m, 1H), 3.61 (m, 2H), 3.25 (m, 1H), 3.03 (m, 1H), 2.57 (m, 1H), 2.39–2.17 (m, 3H), 2.10–1.87 (m, 2H). 1-[(3*R*)-1-Benzylpiperidin-3-yl]-6-(phenylsulfonyl)-1,6-dihydropyrrolo[2,3-*b*][1,2,3]triazolo[4,5-*d*]pyridine (1.70 g, 3.60 mmol) was treated with 2 M aqueous NaOH solution (10 mL) and methanol/THF (1:1, 100 mL) at ambient temperature for 20 min. The mixture was partially concentrated under vacuum and the aqueous residue was extracted with ethyl acetate (3×). The combined extracts were washed with brine, dried with sodium sulfate and concentrated under vacuum to leave an orange residue. Purification by column chromatography on silica gel (gradient: 0–100% ethyl acetate in DCM) afforded 1.17 g (98%) of 1-[(3*R*)-1-benzylpiperidin-3-yl]-1,6-dihydropyrrolo[2,3-*b*][1,2,3]triazolo[4,5-*d*]pyridine (**4**) as a yellow residue. MS (ESI): m+H = 333.2; ^{1}H NMR (400 MHz, DMSO-d_6) δ: 12.34 (s, 1H), 8.99 (s, 1H), 7.55 (t, *J* = 2.8 Hz, 1H), 7.34–7.17 (m, 5H), 6.78 (dd, *J* = 3.5, 1.8 Hz, 1H), 5.10–5.00 (m, 1H), 3.72–3.49 (m, 2H), 3.22 (m, 1H), 2.95 (m, 1H), 2.57–2.50 (m, 1H), 2.32 (m, 1H), 2.26–2.09 (m, 2H), 1.98–1.83 (m, 2H). A solution of **4** (1.16 g, 3.49 mmol) in MeOH (100 mL) was treated with palladium hydroxide (20 wt % on *C*, 244 mg) and ammonium formate (2.20 g, 34.9 mmol) at reflux for 2 h. After cooling the mixture was filtered through Celite and concentrated. The product was purified by column chromatography on silica gel (eluting with 5–10% [2 M NH_3 in MeOH] in DCM) to provide 768 mg (91%) of 1-[(3*R*)-piperidin-3-yl]-1,6-dihydropyrrolo[2,3-*b*][1,2,3]triazolo[4,5-*d*]pyridine (**26**) as a white solid. MS (ESI): m+H = 243.3; ^{1}H NMR (400 MHz, $CDCl_3$) δ: 10.18 (s, 1H), 9.11 (s, 1H), 7.45 (m, 1H), 6.90 (m, 1H), 4.96 (m, 1H), 3.55 (m, 1H), 3.44 (dd, *J* = 12.4, 9.5 Hz, 1H), 3.20–3.13 (dt, *J* = 12.4, 3.9 Hz, 1H), 2.88 (m, 1H), 2.48–2.40 (m, 2H), 2.02–1.94 (m, 1H), 1.86–1.71 (m, 1H). To a stirred solution of **26** (72 mg, 297 μmol) in DCM (15 mL) at 0 °C, cyanoacetic acid (30.0 mg, 357 μmol), *N*-hydroxybenzotriazole (56.0 mg, 416 μmol), 4-(dimethylamino)pyridine (58.0 mg, 475 μmol) and 1-ethyl-3-(3-dimethylaminopropyl)carbodiimide hydrochloride (91.0 mg, 475 μmol) were added. The mixture was then stirred at ambient temperature for 18 h. The crude reaction mixture was purified by column chromatography on silica gel (gradient: 0–6% methanol in DCM) affording 82 mg (92%) of **3** as an off-white solid. LCMS (ESI): m+H = 310.1; ^{1}H NMR was consistent with amide rotamers (400 MHz, DMSO-d_6) δ: 12.38 (br s, 1H), 9.02 (s, 1H), 7.64–7.59 (m, 1H), 7.16–7.08 (m, 1H), 5.28–4.96 (m, 1H), 4.81–4.31 (m, 1H), 4.20–3.70 (m, 3H), 3.36–2.96 (m, 2H), 2.44–1.68 (m, 4H).
22. Racemic *trans* (3-amino-cyclopentyl)-carbamic acid *tert*-butyl ester was prepared following the methods outlined in (a) Li, F.; Brogan, J. B.; Gage, J. L.; Zhang, D.; Miller, M. J. *J. Org. Chem.* **2004**, *69*, 4538; (b) Ranganathan, S.; George, K. S. *Tetrahedron* **1997**, *53*, 3347; (c) Gregson, M.; Ayres, B. E.; Ewan, G. B.; Ellis, F.; Knight, J. Patent WO9417090.; (d) Ray, A. K.; Sigfridsson, E. M.; Linusson, A. S. M.; Sandberg, P. M.; Inghardt, T.; Svensson, A. M.; Brickmann, K. Patent WO2004004726.
23. Synthesis of intermediate **34**: (a) Budzik, B.; Garzya, V.; Shi, D.; Walker, G.; Lauchart, Y.; Lucas, A. J.; Rivero, R. A.; Langmead, C. J.; Watson, J.; Wu, Z.; Forbes, I. T.; Jin, J. *Bioorg. Med. Chem. Lett.* **2010**, *20*, 3545; (b) Synthesis of amines **35b** and **36b**: Dale, G. E.; Pierau, S.; Cappi, M.; Gray, C.; Hubschwerlen, C.; Surivet, J.-P.; Zumbrunn, C. Patent WO2007042325.